Supplementary Information

From the lab to the field: Handheld surface enhanced Raman spectroscopy (SERS) detection of viral proteins

Taylor D. Payne, Stephen J. Klawa , Tengyue Jian, Qunzhao Wang, Sang Hoon Kim, Ronit Freeman*, and Zachary D. Schultz*

Corresponding Authors:

***Zachary D. Schultz -** *Department of Chemistry and Biochemistry, The Ohio State University, Columbus, Ohio 43210, United States; orcid.org/0000-0003-1741-8801; Email: schultz.133@osu.edu*
***Ronit Freeman -** *Department of Applied Physical Sciences University of North Carolina, Chapel Hill, North Carolina 27599, United States; orcid.org/0000-0001-5960-6689; Email: ronifree@email.unc.edu*

Other Authors:
Taylor D. Payne- *payne.737@osu.edu*
Stephen J. Klawa- *sklawa@live.unc.edu*
Tengyue Jian- *jianty@email.unc.edu*
Qunzhao Wang- *qunzhaow@email.unc.edu*
Sang Hoon Kim- *nanro@email.unc.edu*

Table of Contents for Supplementary Figures:

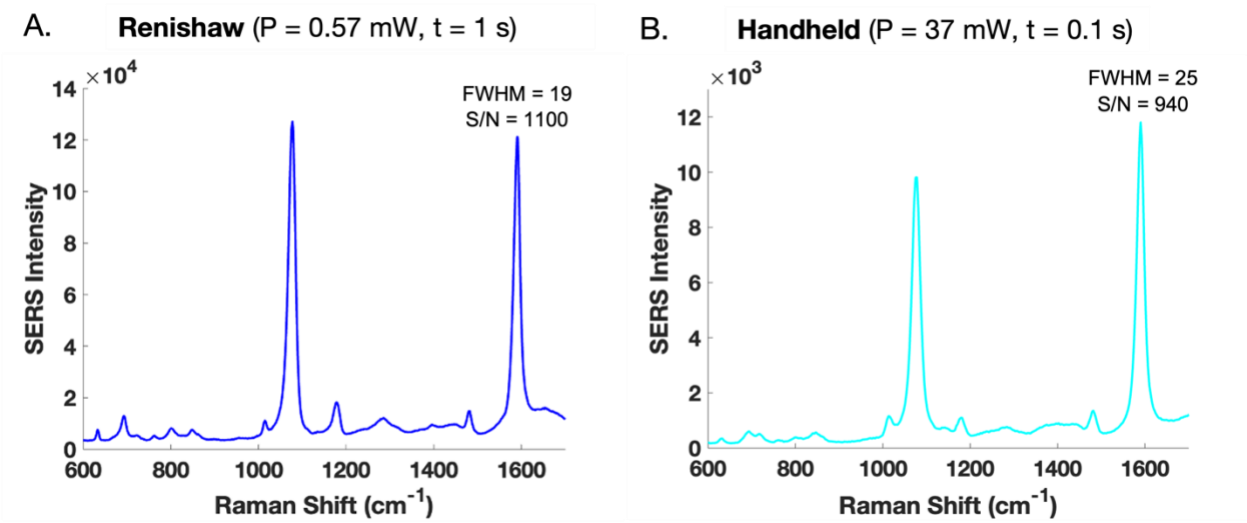

Figure S1. Comparison of SERS signal from a 4-mercaptobenzoic acid (MBA) monolayer on a commercial Silmeco gold substrate using (A) a Renishaw microscope versus (B) a Metrohm handheld spectrometer, demonstrating similar full width at half maximum (FWHM) resolution and signal-to-noise ratio (S/N).

Mercaptobenzoic acid (4-MBA) was prepared in ethanol and used to create a monolayer on commercial gold substrates purchased from Silmeco. These surfaces were used to obtain SERS spectra on both the Renishaw microscope and Metrohm handheld device at 785 nm. S/N was calculated by dividing signal height (from maximum to baseline) by noise height. FWHM was calculated by finding the width of the peak at half the signal height.

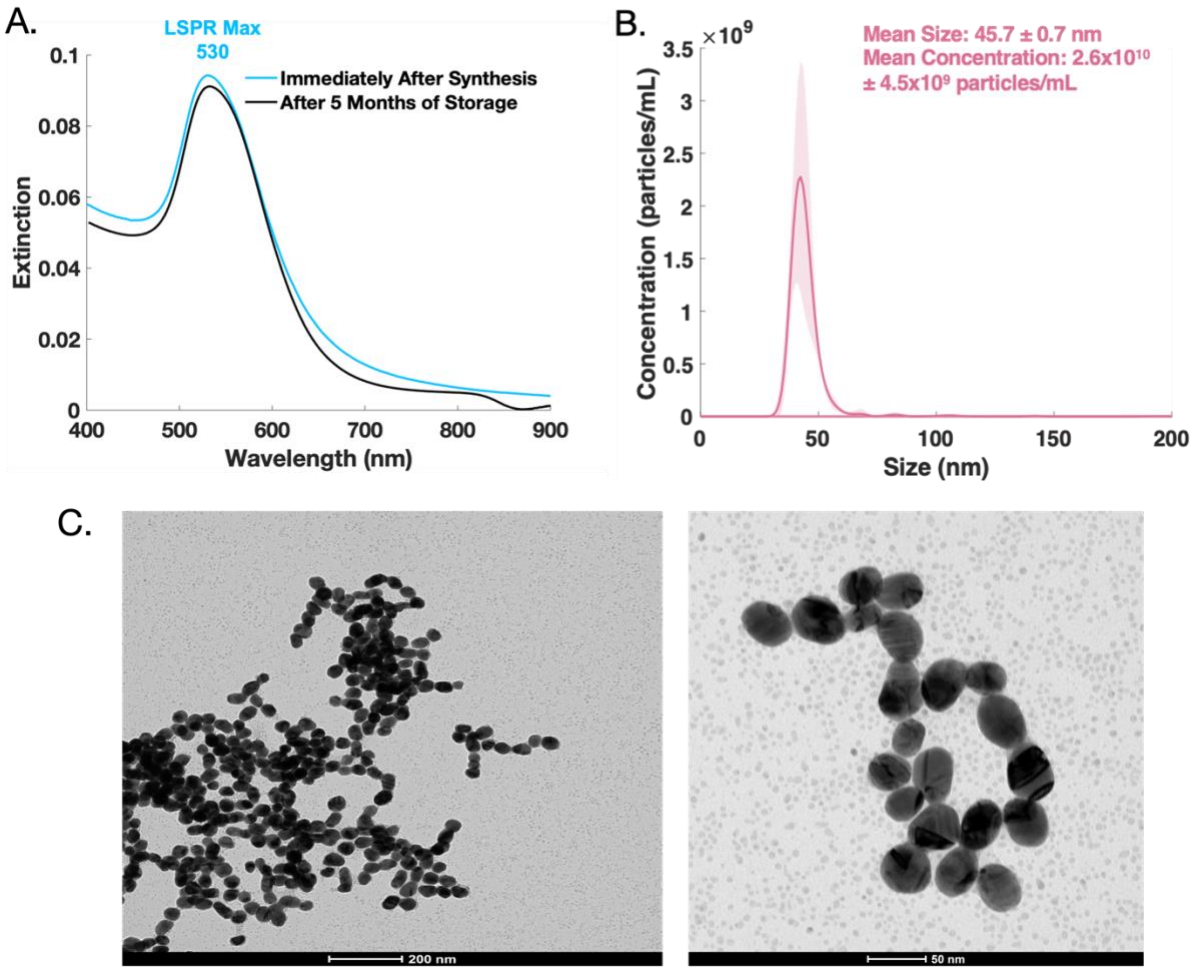

Figure S2: Characterization of synthesized gold nanoparticles. (A) Extinction spectra of gold nanoparticles after synthesis and after 5 months of storage in the dark. Maximum localized surface plasmon (LSPR) at 530 nm. (B) Results from nanoparticle tracking analysis of gold nanoparticles, giving particle size and concentration information. (C) Transmission electron microscopy (TEM) images of gold nanoparticles, showing approximate size and colloidal shape.

Stability of gold nanoparticles was verified by UV-Vis after 5 months of storage in conical tubes covered in aluminum foil. The extinction spectra after 5 months are acquired from undiluted stock solution, while the initial spectra are from 10-fold diluted solution, so the former trace is divided by 10 for comparison. The extinction spectra show no significant shift in the LSPR of the nanoparticles and no significant change in concentration. The very slight peak around 800 nm after storage indicates minimal aggregation.

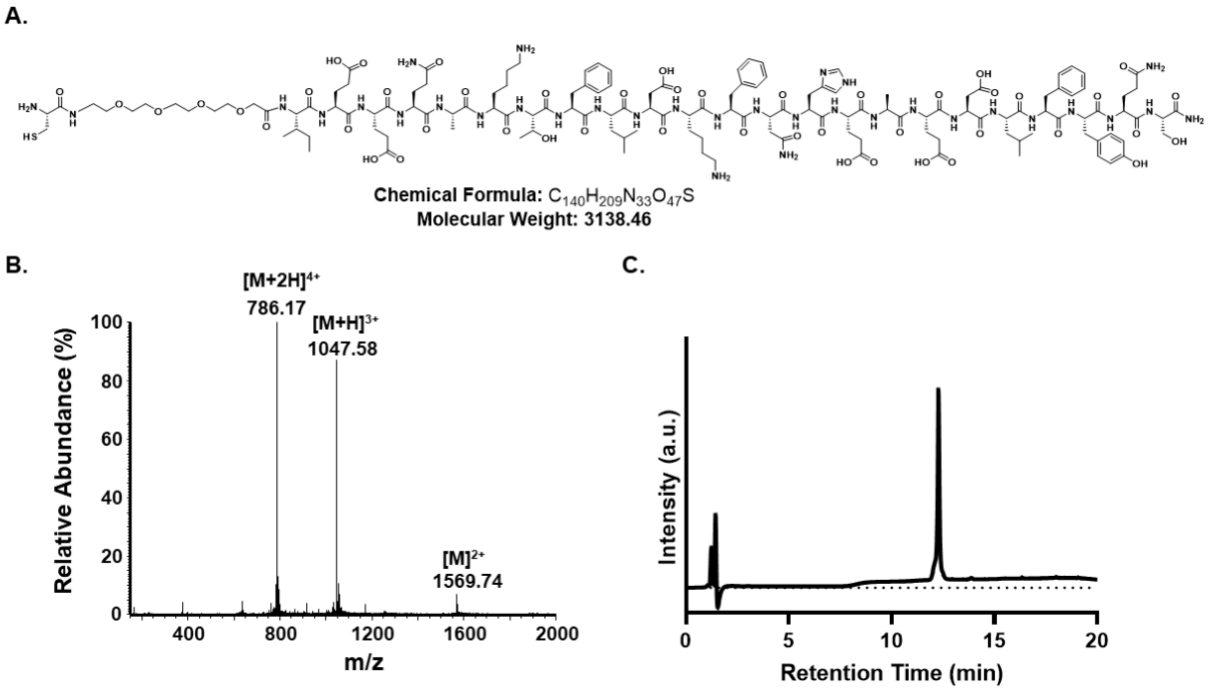

Figure S3. Cys-PEG_4-SBP structure and characterization. (A) Chemical structure of spike binding peptide (SBP). (B) Electrospray ionization mass spectrum (ESI-MS) confirming the identity of the peptide. (C) Analytical HPLC trace monitoring of absorbance at 214 nm to confirm purity of peptide.

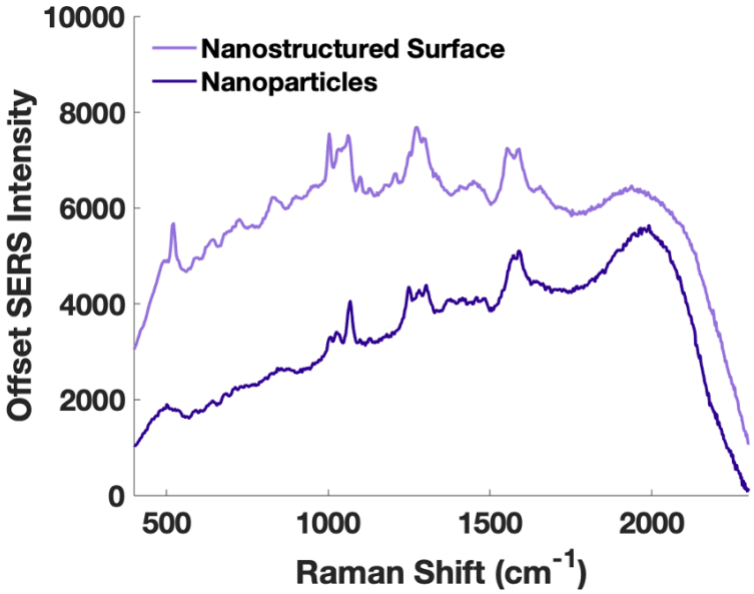

Figure S4. Comparison of handheld SERS signal from peptide on a gold Silmeco surface and on gold nanoparticles. Spectra offset for clarity.

For comparison to nanoparticle samples, a commercial gold substrate (Silmeco), cleaned using heat and sodium borohydride, was shaken overnight in 1 mM peptide solution prepared in 20% DMSO and excess TCEP, then was rinsed with water.

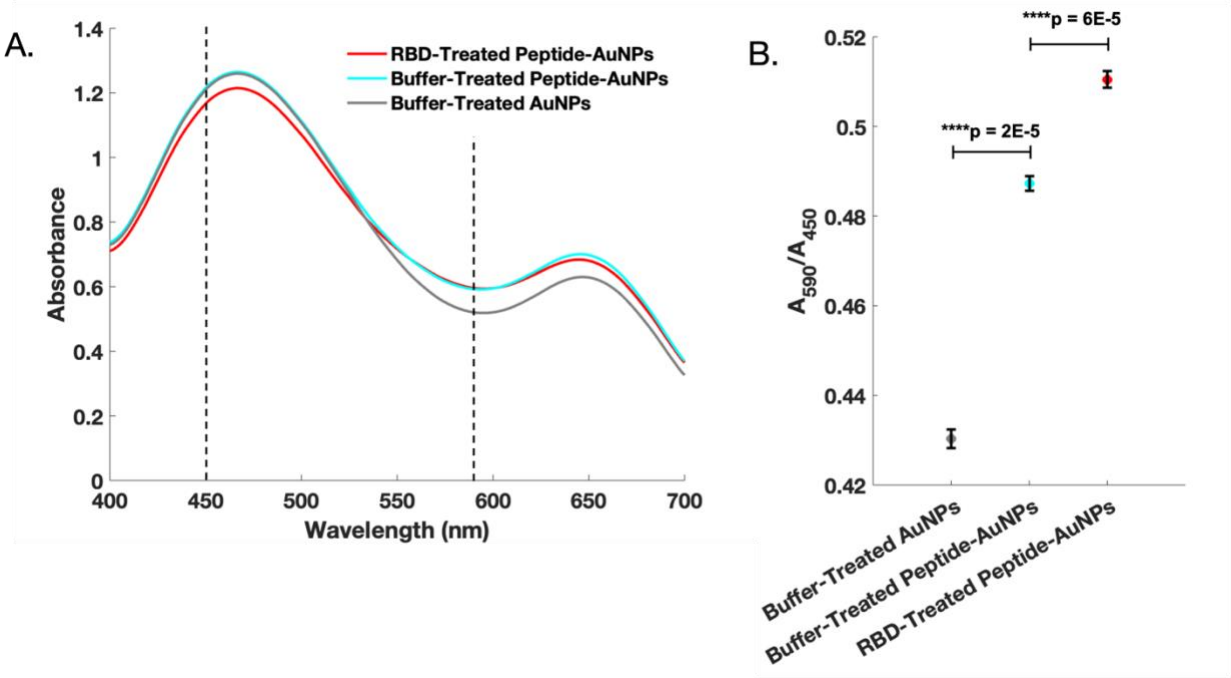

Figure S5. Bradford assay demonstrating functionalization of AuNPs with peptide and subsequent binding of peptide-AuNPs to SARS-CoV-2 RBD. (A) UV-Vis spectra and (B) calculated absorbance ratios showing increase in peptide/protein signal from AuNPs after each treatment.

Prepared solutions of AuNPs treated with RBD buffer mimic, peptide-AuNPs treated with RBD buffer mimic, and peptide-AuNPs treated with 10 µM SARS CoV-2 RBD. Added 20 µL of these samples to 1 mL of 1x Bradford dye and shook at 500 rpm for 5 minutes. Blanked UV-Vis with 1 mL of ultrapure water, then acquired 3 spectra from each solution. Calculated ratios of absorbance peaks at 590 nm and 450 nm, or the ratio of the protein-dye complex to the unbound dye, which extends the linear range of the dye to lower concentrations.[1] One tailed t-tests were performed on the absorbance ratios for the AuNPs vs. peptide-AuNPs and the buffer-treated peptide-AuNPs vs. RBD-treated peptide-AuNPs using the "ttest" function, giving p-values of 2E-4, 6E-5, respectively.

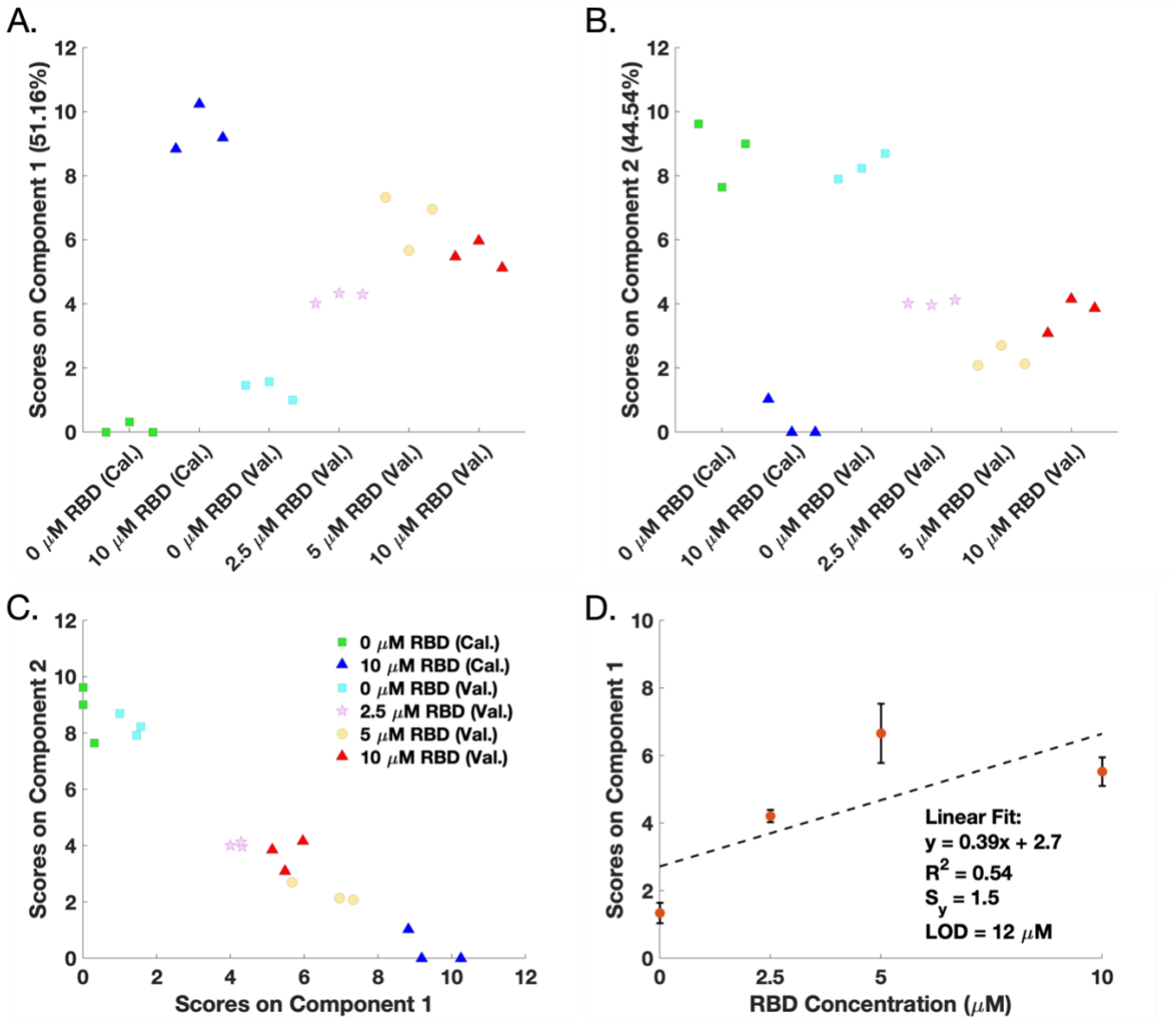

Figure S6. Additional information on construction and validation of multivariate curve resolution (MCR) model. (A) Plot of individual MCR scores for calibration (cal.) and validation (val.) data on component 1. (B) Plot of individual MCR scores for calibration and validation data on component 2. (C) Biplot of component 2 vs. component 1 scores for all calibration and validation data. (D) Attempted calibration curve demonstrated by linear regression model of component 1 scores versus protein concentration. Linear fit is poor, as indicated by $R^2 = 0.54$. Limit of detection (LOD) is calculated as $3S_y/m$.

To obtain calibration data, peptide-AuNPs were adjusted to pH 2 and then shaken for 30 minutes with either 0 μM or 10 μM SARS-CoV-2 RBD. These solutions were centrifuged at 7000 rcf for 30 minutes, and supernatant containing unbound protein was removed. For each solution, 5 μL was placed on a gold-coated well slide, and three Raman spectra were obtained using a Metrohm Mira DS in orbital raster scanning mode (785 nm, 37 mW, 10 s).

To aqcuire validation data, the same procedure was repeated, except with RBD concentrations of 0 μM, 2.5 μM, 5 μM, and 10 μM.

All spectra were imported into MATLAB (version R2019b, Mathworks Inc.) for processing. The spectra were truncated to a Raman Shift (cm^{-1}) range of 400 to 2000 and baselined using airPLS. The spectra were normalized to the height of the 1067 cm^{-1} peak.

Multivariate curve resolution-alternating least squares (MCR-ALS) was selected for modelling to generate loadings representing pure component spectra and scores representing concentration information.The PLS toolbox (version

8.7.1, Eigenvector Research Inc.) was opened in MATLAB, and the "DECOMPOSITION" tab was expanded to select "MCR- Multivariate Curve Resolution". The calibration spectra were loaded into the X-block of the "Calibrate" section of the analysis window. Preprocessing conditions were set to "none", number of components was set to 2, and the model was created. For this model, the Fit (%Model) values indicate that component 1 and component 2 explain 51.16% and 44.54% of the total variance, respectively. The peaks in the loading for component 1 resemble the SERS signal from protein-treated peptide-AuNPs. The bands in the loading for component 2 resemble peptide-AuNPs without protein.

The validation spectra were loaded into the X-block of the "Apply/Validate" section, and the prediction was generated. Samples with higher protein concentration score higher on component 1 and lower on component 2. This also suggests that component 1 represents SERS signal from protein bound to peptide-AuNPs. The loadings and scores from the MCR model were exported as variables in the MATLAB workspace for further processing, such as plotting, calculating averages and standard deviations, and determining p-values. One tailed t-tests were performed on the 10 μM vs. 0 μM, 5 μM vs. 0 μM, and 2.5 μM vs. 0 μM scores using the "ttest" function, giving p-values of 4E-4, 6E-3, and 3E-3, respectively.

Root-mean-square error (RMSE) and unmodelled variance (or sum-squared residuals, RSS) for both the calibration and the validation data were calculated using the "als" function, i.e. "als(X,C)", where X is the dataset and C is the loadings matrix for the component spectra. For the calibration model, RMSE = 4.8 and RSS = 4.3%. For the validation of the model, RMSE = 6.9 and RSS = 4.5%.

Examination of the individual MCR scores from the calibration and validation datasets shows that the 0 μM RBD samples (squares) score slightly, but not significantly, differently from one another ($p = 0.99$). The 10 μM RBD samples (triangles) from the two datasets score significantly differently from one another ($p = 3E-3$). This assay is not quantitative, but differences in the presence of the analyte can be detected qualitatively with statistical significance.

Manufacturer	Product	Laser Wavelength (nm)	Laser Power (mW)	Spectral Resolution (cm^{-1})	Spectral Range (cm^{-1})
Metrohm	Mira DS	785	10-100	8-10	400-2300
Agiltron	PinPointer	785	5-300	9	200-3000
Anton Paar	Cora 100	785	300	10	400-2300
B&W Tek	TacticID-GP Plus	785	300	9	176-2900
B&W Tek	TacticID-N Plus	785	300	9	176-2900
Bruker	Bravo	785	150	10-12	300-3200
Evironics	100 ID	785	300	10	400-2300
Field Forensics	HandyRam II	785	250	10	400-2300
Serstech	100 Indicator	785	300	10	400-2300
Thermo Scientific	First Defender RM	785	250	7-10.5	250-2875
Thermo Scientific	First Defender RMX	785	250	7-10.5	250-2875
Thermo Scientific	Gemini RAMAN	785	250	7-10.5	250-2875
Thermo Scientific	TruNarc	785	250	7-10.5	250-2875

Figure S7. Table of commercially available handheld Raman spectrometers with similar capabilities to the Metrohm Mira DS utilized in this work. Information retrieved from the U.S. Department of Homeland Security.[2]
The spectrometers on this list represent potentially suitable substitutes for the Mira DS, except the Mira DS is the only option equipped with orbital raster scanning (ORS) technology.

References

1. O. Ernst and T. Zor, *JoVE*, 2010, 1918.

2. Handheld Raman Spectrometers, https://www.dhs.gov/science-and-technology/saver/handheld-raman-spectrometers, (accessed July 2023).